Noise-Induced Enantioselection in Chiral Autocatalysis

José M. Cruz and P. Parmananda*

Facultad de Ciencias, Universidad Autónoma del Estado de Morelos, Av. Universidad 1001, Col. Chamilpa, 62209 Cuernavaca, Morelos, Mexico

Thomas Buhse*

Centro de Investigaciones Químicas, Universidad Autónoma del Estado de Morelos, Av. Universidad 1001, Col. Chamilpa, 62209 Cuernavaca, Morelos, Mexico

Received: September 14, 2007; In Final Form: November 20, 2007

Noise added to a chirally autocatalytic model system is usually known to cause mirror-symmetry breaking with statistically equal distributions for the two product enantiomers. We show that if such a system is asymmetrically perturbed by means of a very small undetectable bias in the racemization equilibrium between the two enantiomers, adding Gaussian white noise can lead to an efficient enantioselection. Consequently, within a certain range of the noise amplitude, symmetry breaking gives rise to an entirely biased statistical distribution in favor of one of the enantiomers. In contrast, racemic results will be obtained for the corresponding deterministic case (in the absence of noise). Thus, added noise plays a constructive role by directing the chiral system into a specific enantiomeric direction while being influenced only by a subthreshold asymmetric input. This effect could be of conceptual interest for the impact of weak asymmetric fields on nonlinear chemical reactions.

1. Introduction

The influence of weak chiral forces on asymmetric chemical reactions is of fundamental interest particularly in the search for the origin of biomolecular homochirality.[1] This especially concerns the parity-violating energy difference (PVED) that predicts an exceedingly small but deterministic bias of around 10^{-15} eV between enantiomers of the same kind.[2] Also, other (nonuniversal) chiral factors of comparatively higher potency than the PVED such as circularly polarized light, β-irradiation, or magnetochiral dichroism—all combined with a suitable amplification mechanism[3]—have been associated with the possible cause for the prebiotic evolution toward the enantiomeric homogeneity in nature.[4]

The striking discoveries of chirally autocatalytic systems, like the stirred crystallization of sodium chlorate,[5] the addition of diisopropylzinc to pyrimidine carbaldehydes,[6] or the chiral sign induction by vortex motion,[7] gave evidence of strong amplification mechanisms giving rise to spontaneous enlargement of the smallest enantiomeric excess and mirror-symmetry breaking in laboratory experiments. The later phenomenon, describing a bifurcation scenario that originates from the nonlinear nature of the reaction system,[8] is of particular interest because mirror-symmetry breaking initiates from achiral conditions and leads systematically to a significant product enantiomeric excess in repeated experiments. For a single run, the direction of the enantiomeric outcome cannot be predicted, but for a large number of experiments, a symmetric and bimodal product distribution around the two opposite optically active states is usually obtained.[5,9]

Any effect by the PVED, which could be expected to cause a slight asymmetric shift in these product distributions, has not been detected so far in the above systems, although stronger chiral fields such as, for instance, the irradiation with β-particles or positrons during the crystallization of sodium chlorate,[10] circularly polarized light in the diisopropylzinc addition to pyrimidine carbaldehydes,[11] or vortex motion during the aggregation of soft condensed materials[7] can drive the outcome significantly into a predictable direction. The lack of any detectable response toward tiny but systematic asymmetric perturbations is generally attributed to the presence of inevitable fluctuations, that is, reaction noise, which can readily overshadow weak chiral fields like the PVED and consequently lead to symmetrical results in the product distributions of experimental systems.

Theoretical studies based on kinetic networks that include chiral autocatalysis have shown that added noise or internal numerical noise can lead to an almost homochiral state starting from achiral conditions in simulations.[12] As expected, the probability distribution in these attempts remained symmetrical. Hence, random noise has been described so far to trigger mirror-symmetry breaking with a statistical outcome. In contrast, in the present work, we give numerical evidence that superimposed noise can divulge previously untraceable asymmetry in a chirally autocatalytic system. This nontrivial result is observed only for a finite interval of the noise amplitude. This noise-provoked effect resembles the various examples in which random noise can play a constructive instead of a destructive role.[13]

* To whom correspondence should be addressed. Tel: +527773297020. Fax +527773297040. E-mail: punit@servm.fc.uaem.mx (P.P.); Tel/Fax: +527773297997. E-mail: buhse@uaem.mx (T.B.).

Here, we evaluate the impact of random noise on a chirally autocatalytic model system that is under the influence of continuous asymmetric perturbations that we understand as a subthreshold deterministic input. Random noise will be assessed for its potential to amplify such chiral perturbations with the possible effect on the resulting probability distributions of the generated enantiomers.

2. Model

We used a generic kinetic model derived from the classical Frank scheme[14] of chiral autocatalysis in which we considered, additionally, the racemization between the enantiomers R and S, step 6

$$A \rightarrow R \quad k_0 \tag{1}$$

$$A \rightarrow S \quad k_0 \tag{2}$$

$$A + R \rightarrow 2R \quad k_1 \tag{3}$$

$$A + S \rightarrow 2S \quad k_1 \tag{4}$$

$$R + S \rightarrow P \quad k_2 \tag{5}$$

$$R \leftrightarrow S \quad k_3, k_4 \tag{6}$$

Here, A stands for the achiral substrate, R and S stand for the enantiomeric autocatalytic species, and P stands for an inactive product. Steps 1 and 2 denote the direct formation of the product enantiomers and steps 3 and 4 their essential autocatalytic generation as the core of the chiral enlargement. Step 5 represents enantiomeric cross-inhibition, yielding an optically inactive product as a necessary element to achieve sustained chiral amplification. Although the above model is of general nature, its key features such as chiral autocatalysis and mutual inhibition between the enantiomers have been demonstrated just to be the essential ingredients for experimental realizations of spontaneous chiral amplification and mirror-symmetry breaking. This concerns the few known examples involving crystallization from solution[5] or melt,[15] aggregation of soft condensed materials,[7,16] cluster formation,[17] or metal−organic synthesis under homogeneous conditions.[6,12b]

Taking into further account an open-system evolutionary scenario and the realistic presence of product racemization,[18] which directs the system in its long-term evolution into a racemic equilibrium state if k_3 and k_4 are equally valued, CSTR conditions have been assumed in which a constant inflow of A and a corresponding outflow of the reaction mixture occurs. These considerations lead to the following set of differential equations as used for our approach
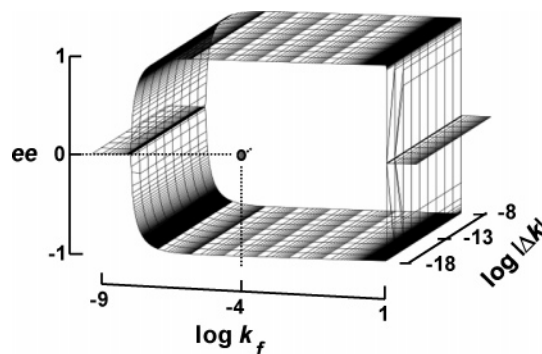
$$d[A]/dt = -2k_0[A] - k_1[A]([R] + [S]) + k_f([A]_0 - [A]) + \xi_{(1,2,3,4,5)} \tag{7}$$

$$d[R]/dt = k_0[A] + k_1[A][R] - k_2[R][S] - k_3[R] + k_4[S] - k_f[R] + \xi_{(2,3,4,5,1)} \tag{8}$$

$$d[S]/dt = k_0[A] + k_1[A][S] - k_2[R][S] - k_4[S] + k_3[R] - k_f[S] + \xi_{(3,4,5,1,2)} \tag{9}$$

$$d[P]/dt = k_2[R][S] - k_f[P] + \xi_{(4,5,1,2,3)} \tag{10}$$

where k_f denotes the flow rate constant and $[A]_0$ the inflow concentration of the achiral substrate. The ξ stands for the added

Figure 1. Region in the parameter space of the flow rate constant k_f and asymmetric perturbation $|\Delta k|$ in which a stationary nonzero enantiomeric excess (ee) in the absence of noise is obtained; $[A]_0 = 1$ M, $[R]_0 = [S]_0 = 0$, $k_0 = 10^{-5}$ s^{-1}, $k_1 = 1$ M^{-1}·s^{-1}, $k_2 = 10$ M^{-1}·s^{-1}, $k_3 = 10^{-4}$ s^{-1}, and k_4 has been varied. As indicated by the filled circle, the set points for later simulations in which $\xi \neq 0$ were chosen outside of this region at $k_f = 0.4$ s^{-1} and $|\Delta k| < 1.97 \times 10^{-18}$ s^{-1}.

noise that was produced by a random number generator with the output symmetrically distributed over the interval $[-1,1]$ corresponding to Gaussian white noise, implying that all frequencies appear with equal probabilities and that the chosen set point remains on an average invariant. Five different noise sequences with the same statistical properties were sequentially permutated over the four differential eqs 7−10, giving rise to 120 individual sets of differential equations used in our simulations.

The effect of a continuous asymmetric perturbation was introduced by the condition $k_3 \neq k_4$. In this case, the steady-state reaction coefficient of the equilibrium R ↔ S remains systematically shifted, favoring one enantiomer over the other. This could mimic for instance the presence of a chiral factor giving rise to an energy difference between the two enantiomers. For simplicity, the steps 1 and 2 as well as 3 and 4 were considered as symmetric and consequently did not show any differences in the rate parameters for the processes related to R or S, respectively.

Numerical integrations were performed using a fourth-order Runge−Kutta algorithm with fixed step size. Repeated simulations verified that for the precision of the chiral asymmetry considered, round-off errors did not affect the results.

3. Numerical Results and Discussion

By allowing variations in the flow rate constant k_f and the asymmetric perturbation $\Delta k = k_3 - k_4$ as well as by keeping k_0, k_1, and k_2 at fixed values and the noise at zero, the parameter space of the model describes a domain in which chiral amplification occurs (Figure 1). The lower limit of k_f, after which a sharp transition into the optically active state takes place, is readily explained by the racemization process that causes zero enantiomeric excess if the system approaches batch conditions. The upper limit of k_f at which the racemic state is re-established can be understood by the reactor washout due to the highly elevated inflow of A. Under these conditions, the stationary concentration of A remains about at its initial value, and a very small amount of R and S is generated. On the contrary, in the amplification domain, the stationary concentration of A drops to a very small value, and those of R and S rise significantly.

In the amplification domain given by k_f, another bifurcation scenario can be observed by variation of Δk. If $\Delta k = 0$, the system stays entirely symmetric, and at any k_f, a racemic result is obtained. However, chiral amplification in our simulations

Letters

J. Phys. Chem. A, Vol. 112, No. 8, 2008 **1675**

TABLE 1: Enantiomeric Product Distribution for Various Values of the Noise Amplitude and Asymmetric Perturbation Δk. Each Entry for the R and S Distribution is Based on 120 Individual Numerical Simulations in Which Distinct Combinations of 5 Different Noise Seeds over the 4 Differential Eqs 7−10 Have Been Used; Same Initial Conditions and Rate Parameter Values as Those in Figure 1

noise amplitude $\times 10^{-13}$ (M·s^{-1})	$\Delta k = 0$		$\Delta k = 5.0 \times 10^{-19}$ s^{-1}		$\Delta k = 1.9 \times 10^{-18}$ s^{-1}	
	R	S	R	S	R	S
0	0	0	0	0	0	0
3	0	0	0	0	0	0
3.13	0	0	0	0	0	12
3.14	0	0	0	0	0	24
3.15	0	0	0	24	0	24
3.16	24	24	24	24	0	24
3.17	24	24	24	24	0	24
6.6	24	24	24	24	24	24
6.7	42	42	36	42	24	42
6.9	42	42	42	42	42	42
7	48	48	42	54	36	54
10	54	54	54	54	54	60
20	54	54	54	54	54	54
25	54	54	54	54	54	60
30	60	60	60	60	54	60
40	60	60	60	60	60	60

Figure 2. Degree of asymmetry (S − R)/(S + R) × S versus noise amplitude indicating an optimum noise level at which the induced enantioselection shows the highest efficiency; $\Delta k = 1.9 \times 10^{-18}$ s^{-1}, the same conditions as those in Figure 1, if S + R = 0 ⟹ (S − R)/(S + R) × S = 0.

did not occur for any situation at which $|\Delta k| > 0$ but rather after a tiny critical value of $|\Delta k| \approx 1.97 \times 10^{-18}$ s^{-1} (at $k_f = 0.4$ s^{-1}). Hence, during the deterministic simulations, exceedingly small chirally asymmetric induction remained undisclosed while any value of $|\Delta k|$ higher than the above threshold directed each simulation into the preferred enantiomeric direction, that is, for positive values of Δk into the S direction and for negative values into the R direction without any exception. By approaching the bifurcation point, the simulations showed an "all or none" behavior practically without the occurrence of intermediate values between 0 and 100% for the enantiomeric excess. Further increasing $|\Delta k|$ to higher values obviously did not change the amplification behavior and reduced the transient times for reaching stationary concentrations.

To evaluate noise-induced symmetry breaking starting from achiral or virtually achiral initial conditions ($0 \leq \Delta k < 1.97 \times 10^{-18}$ s^{-1}), we selected a set of parameters as marked in Figure 1 that describes a region just outside of the amplification domain with respect to Δk but inside of the window given by the flow rate constant ($k_f = 0.4$ s^{-1}). Table 1 shows the results in each case of 120 successive simulations and under gradual variation of the noise amplitude between 3.0×10^{-13} and 4.0×10^{-12} M·s^{-1}.

Reviewing the case of $\Delta k = 0$, at low noise amplitudes and after 120 individual simulations, the system behaves like that in the deterministic case, where no symmetry breaking occurs. However, at a higher noise level, the onset of chiral symmetry breaking takes place, giving rise to a statistically symmetric (bimodal) distribution of the R and S results with an enantiomeric excess of almost 100% in each case. Increasing the noise level leads to a rise in the symmetry-breaking probability so that symmetry breaking happens in every individual simulation after a noise amplitude $\geq 3.0 \times 10^{-12}$ M·s^{-1}, yielding 60 results in favor of R and 60 in favor of S. Evidently, during all of these attempts, the enantiomeric direction of each single simulation remained unpredictable. An identical result has been observed for a vanishingly small asymmetric perturbation of $\Delta k = 1.0 \times 10^{-20}$ s^{-1}.

In contrast, the selected cases at which $\Delta k = 5.0 \times 10^{-19}$ and 1.9×10^{-18} s^{-1} show a particularly interesting feature; within a certain interval of the noise amplitude, the small
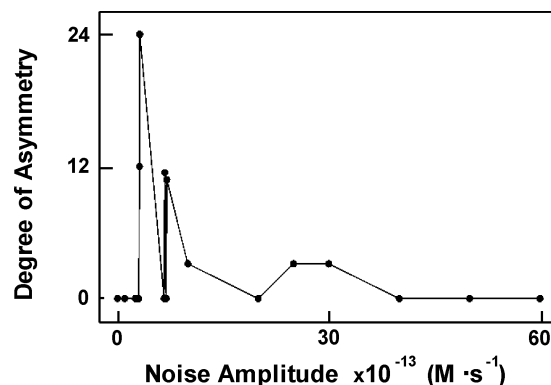
asymmetric perturbations Δk, being concealed at a subthreshold level in the deterministic simulations, are now revealed by the added noise, and efficient enantioselection occurs. This notable effect is reflected by an asymmetric probability distribution of the R and S results that again individually reach an enantiomeric excess of almost 100% in each case. Since Δk has been chosen as positive and $\Delta k = k_3 - k_4$, S results are favored over the R ones, but control simulations showed just the same results for the mirror-image scenario.

The above effect is further illustrated in Figure 2. At a low noise level, the system displays no symmetry breaking at all; then, by increasing the noise amplitude, symmetry breaking starts and gives rise to an entirely biased product distribution in favor of S that leads to a maximum in the asymmetric distribution. Further increasing the noise level results in the successive decrease of this distribution and in an increase of the overall symmetry-breaking probability until a symmetric 60:60 product distribution like that in the former case of $\Delta k = 0$ is reached.

In conclusion, we have shown that noise added to a chirally autocatalytic system can expose an asymmetric perturbation that can be so small as to remain untraceable in the absence of noise. This new feature is believed to have further impact on the fundamental question of weak asymmetric forces and their consequences for chiral systems as well as give evidence of an additional manifestation of the constructive role of noise in nonlinear reaction systems.

References and Notes

(1) (a) Bonner, W. A. *Origins Life Evol. Biosphere* **1991**, *21*, 59−111. (b) Keszthely, L. *Q. Rev. Biophys.* **1995**, *28*, 473−507. (c) Sandars, P. G. H. *Int. J. Astrobiol.* **2005**, *4*, 49−61.

(2) (a) Hegstrom, R. A.; Rein, D. W.; Sandars, P. G. H. *J. Chem. Phys.* **1980**, *73*, 2329−2341. (b) MacDermott, A. J. *Origins Life Evol. Biosphere* **1995**, *25*, 191−199.

(3) Kondepudi, D. K.; Asakura, K. *Acc. Chem. Res.* **2001**, *34*, 946−954.

(4) (a) Avalos, M.; Babiano, R.; Cintas, P.; Jiménez, J. L.; Palacios, J. C.; Barron, L. D. *Chem. Rev.* **1998**, *98*, 2391−2404. (b) Rikken, G. L. J. A.; Raupach, E. *Nature* **2000**, *405*, 932−935.

(5) Kondepudi, D. K.; Kaufman, R. J.; Singh, N. *Science* **1990**, *250*, 975−976.

(6) Soai, K.; Shibata, T.; Morioka, H.; Choji, K. *Nature* **1995**, *378*, 767−768.

(7) Ribó, J. M.; Crusats, J.; Sagués, F.; Claret, J.; Rubires, R. *Science* **2001**, *292*, 2063−2066.

(8) Kondepudi, D. K.; Nelson, G. W. *Phys. Rev. Lett.* **1983**, *50*, 1023−1026.

(9) Soai, K.; Sato, I.; Shibata, T.; Komiya, S.; Hayashi, M.; Matsueda, Y.; Imamura, H.; Hayase, T.; Morioka, H.; Tabira, H.; Yamamoto, J.; Kowata, Y. *Tetrahedron: Asymmetry* **2003**, *14*, 185−188.

(10) Pagni, R. M.; Compton, R. N. *Cryst. Growth Des.* **2002**, *2*, 249−253.

(11) Kawasaki, T.; Sato, M.; Ishiguro, S.; Saito, T.; Morishita, Y.; Sato, I.; Nishino, H.; Inoue, Y.; Soai, K. *J. Am. Chem. Soc.* **2005**, *127*, 3274−3275.

(12) (a) Todorović, D.; Gutman, I.; Radulović, M. *Chem. Phys. Lett.* **2003**, *372*, 464−468. (b) Rivera Islas, J.; Lavabre, D.; Grevy, J. M.; Hernández Lamoneda, R.; Rojas Cabrera, H.; Micheau, J. C.; Buhse, T. *Proc. Natl. Acad. Sci. U.S.A.* **2005**, *102*, 13743−13748. (c) Hochberg, D.; Zorzano, M. P. *Chem. Phys. Lett.* **2006**, *431*, 185−189.

(13) (a) Gammaitoni, P.; Hanggi, P.; Jung, P.; Marchesoni, F. *Rev. Mod. Phys.* **1998**, *70*, 223−288. (b) Amemiya, T.; Ohmori, T.; Nakaiwa, M.; Yamaguchi, T. *J. Phys. Chem. A* **1998**, *102*, 4537−4542. (c) Escalera Santos, G. J.; Rivera, M.; Parmananda, P. *Phys. Rev. Lett.* **2004**, *92*, 230601.

(14) Frank, F. C. *Biochim. Biophys. Acta* **1953**, *11*, 459−463.

(15) Kondepudi, D. K.; Laudadio, J.; Asakura, K. *J. Am. Chem. Soc.* **1999**, *121*, 1448−1451.

(16) Rubires, R.; Farrera, J. A.; Ribó, J. M. *Chem.—Eur. J.* **2001**, *7*, 436−446.

(17) Asakura, K.; Ikumo, A.; Kurihara, K.; Osanai, S.; Kondepudi, D. K. *J. Phys. Chem. A* **2000**, *104*, 2689−2694.

(18) Kondepudi, D.; Prigogine, I. *Modern Thermodynamics*; Wiley: New York, 1998; pp 431−438.